CARBON 56 (2013) 1–11

Available at www.sciencedirect.com

SciVerse ScienceDirect

journal homepage: www.elsevier.com/locate/carbon

Review

Multi-scale mechanical improvement produced in carbon nanotube fibers by irradiation cross-linking

T. Filleter [a], H.D. Espinosa [b,*]

[a] Department of Mechanical & Industrial Engineering, University of Toronto, 5 King's College Rd., Toronto, ON, Canada M5S 3G8
[b] Department of Mechanical Engineering, Northwestern University, 2145 Sheridan Rd., Evanston, IL 60208, USA

ARTICLE INFO

Article history:
Received 24 September 2012
Accepted 8 December 2012
Available online 19 December 2012

ABSTRACT

Fibers and yarns based on carbon nanotubes (CNT) are emerging as a possible improvement over more traditional high strength carbon fibers used as reinforcement elements in composite materials. This is driven by a desire to translate the exceptional mechanical properties of individual CNT shells to achieve high performance macroscopic fibers and yarns. One of the central limitations in this approach is the weak shear interactions between adjacent CNT shells and tubes within macroscopic fibers and yarns. Furthermore, the multiple levels of interaction, e.g., between tubes within a multi-walled CNT or between bundles within a fiber, compound the problem. One promising direction to overcome this limitation is the introduction of strong and stiff cross-linking bonds between adjacent carbon shells. A great deal of research has been devoted to studying such cross-linking by the irradiation of CNT based materials using either high energy particles, such as electrons, to directly covalently cross-link CNTs, or electromagnetic irradiation, such as gamma rays to strengthen polymer cross-links between CNT shells and tubes. Here we review recent progress in the field of irradiation-induced cross-linking at multiple levels in CNT based fibers with a focus on mechanical property improvements.

Contents

* *Corresponding author.*
E-mail address: espinosa@northwestern.edu (H.D. Espinosa).
0008-6223/$ - see front matter
http://dx.doi.org/10.1016/j.carbon.2012.12.016

1. Experimental and theoretical demonstration of weak shear interactions between CNT tubes and shells

Despite the great potential of applying CNTs in composite materials [1–8], an intrinsic limitation in directly scaling up the exceptional mechanical properties of CNTs [9,10] to macroscopic fibers and yarns exists in the form of weak interfacial shear properties between adjacent CNT shells. The same unique nature of in plane sp^2 bonding in CNTs, which achieves high mechanical strength and stiffness, also leads to weak out of plane bonding. This is exemplified in graphite which exhibits some of the best solid lubricating properties found in nature due to inter-planar shear. Such weak inter-plane bonding is evident from theoretical predictions of interfacial properties (cohesion energy, interfacial shear strength, etc.) of stacked graphitic sheets and tubes. The cohesion energy (or interlayer binding energy) in graphite has been calculated by assuming a Lennard–Jones like potential to be 0.33 J/m^2 [11]. A variety of experimental studies have demonstrated interlayer cohesion energies for sp^2 bonded carbon based materials consistent with this theoretical prediction including; multiwalled carbon nanotube (MWCNT) shells (0.198–0.21 J/m^2) [12,13], CNT bundles (0.1–0.6 J/m^2) [25], and graphite (0.26–0.37 J/m^2) [11,14]. Similarly the interfacial shear strength (IFSS) of bare CNT shell–shell interfaces has been experimentally estimated to be as low as 0.05–0.3 MPa [9,12,15]. To put these interfacial properties in perspective the IFSS within typical high performance fiber reinforced composites, such as aramid/epoxy and carbon fiber/epoxy composites, is two to three orders of magnitude higher, on the order of tens of MPa [16].

1.1. Shells within MWCNTs

The weak interfacial shear properties that exist between shells within individual CNTs was experimentally elucidated through in situ transmission electron microscopy (TEM) and scanning electron microscopy (SEM) shear experiments. Cumings and Zettl [17] conducted one of the first direct demonstrations of the sword-in-sheath failure and weak interfacial shear between the inner shells of a MWCNT. In this study the inner shells of a MWCNT were pulled out of the outer shell in a reversible process in situ TEM (Fig. 1c). They estimated the van der Walls (vdW) interlayer force to be approximately 2.3×10^{-14} N/atom. They also demonstrated that the pulled out inner shells tend to be pulled back in, due to the vdW interactions between the inner and outer shells, with nearly zero energy dissipation. Subsequent pull-out studies by Kis et al. [12], which utilized an AFM force sensor in situ a TEM, estimated that the interlayer shear was dominated by van der Walls interactions with a corresponding interlayer shear strength of <0.05 MPa and an interlayer cohesion energy of 33 meV/atom [12], in good agreement with estimates determined from an energy analysis of bare collapsed MWCNTs [13].

The shear interactions between shells of a MWCNT was also quantified by Yu et al. [15] using a similar AFM cantilever based method in situ a SEM. In these experiments, the outer shell of a MWCNT was first pulled in tension, leading to the outer shell rupture followed by the controlled pull out of the inner MWCNT shells. The pull out force measured by Yu et al. was described as being composed of two components: (1) the shear interaction between shells, and (2) the capillary effect and edge interactions by dangling bonds at the end of the MWCNTs. In their study the static shear strength was estimated to be 0.08–0.3 MPa (corresponding to an experimental force of 85–219 nN), and the combined capillary and edge effect was measured to contribute 80–150 nN, dominating the experimentally observed forces.

The low force required for sliding between adjacent MWCNT shells was further investigated by Espinosa and coworkers using a MEMS platform in situ a TEM [9,21] (Fig. 1d). They measured an even lower average post failure force of 35 nN required to pullout the 11 inner shells of a 14 nm diameter MWCNT with respect to the outer shell. Moreover, using DFT, TB-DFT, and reactive force fields they investigated computationally the interaction between tube shells [9,21].

1.2. CNTs within bundles

Similarly weak interfacial interactions have also been predicted and measured experimentally at the next structural level of hierarchy in CNT fibers; CNT bundles. In-situ SEM tensile experiments conducted on individual single- (SWCNT) and double-walled (DWCNT) carbon nanotube bundles have revealed a similar sword-in-sheath failure mechanism in which inner CNTs within bundles pull out with respect to an outer shell of CNTs [6,22,23].

Yu et al. [23] conducted tensile tests on SWCNT bundles in situ SEM using an AFM cantilever based method. Their tensile test data was best fitted by a model, which assumed that only the outer perimeter of SWCNTs in the bundle carried the load, consistent with a sword-in-sheath failure. Although they did not measure the force required to pullout inner SWCNTs from the bundles, the SEM images of the bundles after tensile failure also suggested this mode of failure. More recently a novel method of in situ SEM peeling between two SWCNT bundles was used to measure an adhesion energy

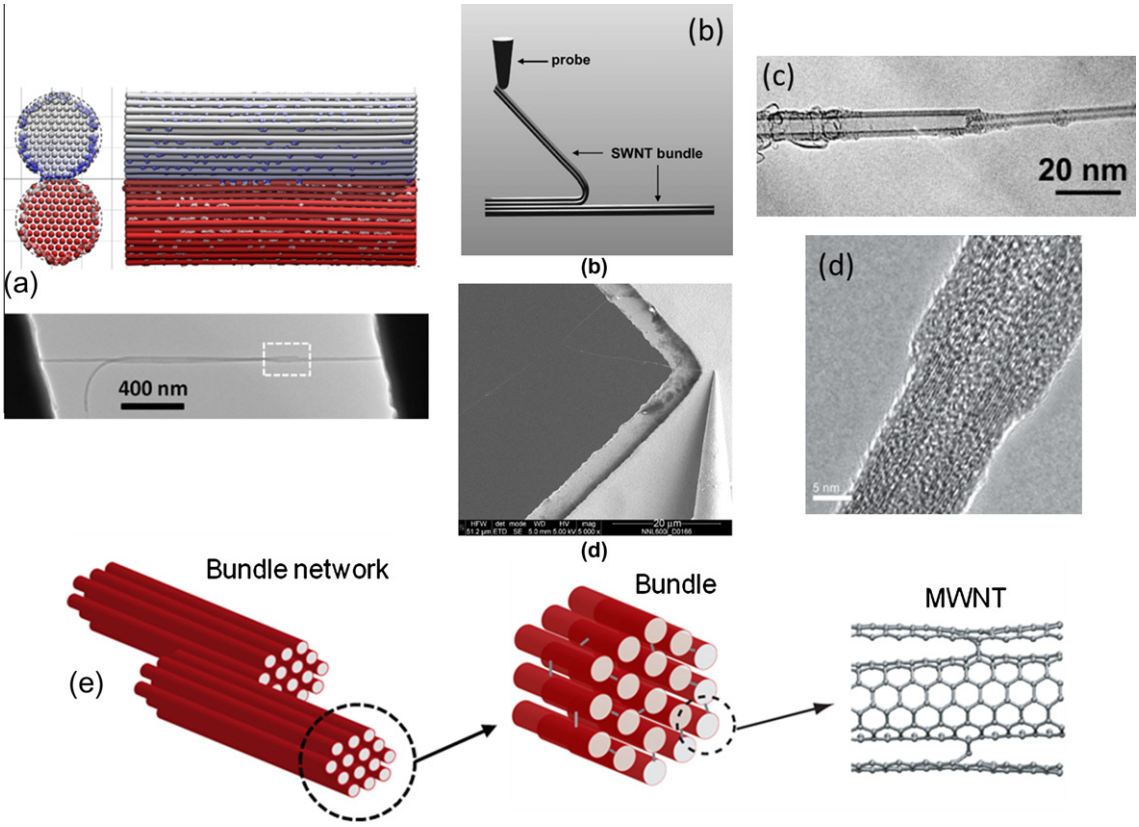

Fig. 1 – Shear interfaces at multiple length scales within CNT based fibers. (a) DWCNT bundle-bundle interfaces. Adapted from [18]. (b) SWCNT-SWCNT interface within a SWCNT bundle. Adapted from [19]. (c) and (d) MWCNT shell-shell interfaces. Adapted from [17] [9]. (e) Schematic of the different CNT yarn length scales. Adapted from [8].

of 0.12–0.16 nJ/m [19] (Fig. 1b); however, the width of the contact between the two bundles was not reported, therefore the cohesion energy per unit area is unknown, making comparison with other studies difficult.

The force required to slide adjacent DWCNTs within bundles was measured recently by Filleter et al. [22]. In this study a normalized pullout force of 1.7 ± 1.0 nN/CNT-CNT interaction was measured for sliding of a smaller inner bundle of DWCNTs out of a larger outer shell of DWCNTs. This force translates to a lower limit estimate of the average interfacial shear strength of approximately 7.8 MPa. This estimation considers as the interfacial area the continuous cylindrical surface area of the small inner bundle of DWCNTs that is pulled out in the experiment ($A = \pi^*l^*d$, where l is the DWCNT overlap length and d is the inner bundle diameter). The true shear strength of the interface is expected to be significantly higher as the interfacial area is not continuous, but instead composed of discrete CNT-CNT interfaces, and the interfacial shear stress in the axial direction is not uniform [24]. Through comparison with molecular mechanics (MM) and density functional theory (DFT) simulations of sliding between adjacent CNTs in bundles it was identified that factors contributing to the pullout force (in units of nN/CNT-CNT interaction) included the creation of new CNT surfaces (<0.4), carbonyl functional groups terminating the free ends (<0.16), corrugation of the CNT-CNT interaction (~0.1), and polygonilization of the CNTs in the bundle (~0.02–0.08). In addition a top down analysis of the experimental results revealed that greater than one half of the pullout force was due to dissipative forces. This finding of behavior at the CNT bundle level significantly differs from the behavior of pullout in individual MWCNTs for which dissipation is found to be negligible [17]. These findings suggest that the bundle hierarchical level may play an important role in energy dissipation and toughness of CNT fibers and yarns. This is also consistent with the greater shear strength measured for bundle pullout (~7.8 MPa) as compared to MWCNT shell pullout (~0.05–0.3 MPa).

Yang et al. [25] experimentally investigated the friction within macroscopic SWCNT fibers by loading large fibers in tension. In contrast to the previously discussed studies here the fibers were of very large diameter (10's μm) and long lengths (~3 mm). It should be noted that the authors of Ref. [25] used the term "bundles" to describe the material under study, however, that term is more typically used to refer to close-packed, aligned CNT structures with diameters on the order of 10's of nm (Fig. 1). During the tensile loading, they monitored both the elastic behavior and the inelastic behavior of the yarns due to SWCNTs sliding on each other. They estimated the cohesive energy per unit area of the SWCNTs to be in the range of 0.1–0.6 J/m^2, by normalizing the friction energy (dissipated during the plastic deformation) by the change in the contact area between the bundles. While this method can be used to obtain an average value for the

cohesive energy between SWCNTs, it suffers from uncertainties in the estimation of the edge effect and the true contact area between SWCNTs. In addition the analysis assumes close packing of SWCNTs in the large diameter fibers, which leads to further uncertainties.

2. Irradiation methods for cross-linking of graphite and CNTs

2.1. High energy particle irradiation

One approach which can increase the shear strength of the weak CNT interfaces described in the previous section is to introduce interlayer covalent bonding between carbon atoms of adjacent graphitic layers through particle irradiation [9,26–30]. The effect of radiation on graphite has been a topic of interest for many years [31–33]. For example, in 1963 Goggin demonstrated that the Young's modulus of graphite could be increased by electron irradiation and thermal annealing [33]. Radiation of carbon nanostructures, such as CNTs, have only more recently been investigated due to the potential beneficial effects. Such an approach requires locally modifying the in-plane sp^2 bonding to sp^3 type bonding at specific sites within the CNT material. The benefit to the interfacial shear strength can be understood by considering the relative single bond energies of the sp^3 C–C bonds found in diamond (~0.88 eV/atom) [34] as compared to the interplanar binding energy of graphite sheets (~0.02 eV/atom) [35]. Recently, irradiation with high energy particles, including electrons, protons, and ions, has been both theoretically and experimentally demonstrated as an effective method to introduce interlayer covalent bonding in graphite and CNT materials by the formation of cross-linking defects in the graphitic structures [9,21,27,28,36–38]. High energy electrons, in particular, have been studied extensively with application to mechanical property improvements achieved through cross-linking CNT shells and tubes [9,21,27,30,31,37]. For a general review of the effects of irradiation on other nanostructures, the reader is referred to the following review articles [39,40].

2.1.1. Type and role of defects

Irradiation of CNTs and graphite layers with high energy electrons leads to the formation of atomic-scale defects due to the transfer of energy from the incident electron to the carbon atoms in the graphitic structures. The creation of a defect requires that the target atom acquires sufficient kinetic energy to be displaced from its original position in the lattice. The energy thresholds for electron irradiation induced defect creation in graphite and CNT will be discussed further in Section 2.1.2.

Defects formed by electron irradiation in graphite and CNTs can be in the form of point defects [21,41] (Fig. 2a) or larger dimension defects such as dislocations and voids in graphitic layers [42] (Fig. 2b). For applications aimed at improving the mechanical behavior of CNT materials, point defects that bridge adjacent layers are most desirable as larger in plane defects can significantly reduce the intrinsic mechanical properties of the CNT shells. MM simulations conducted by Mielke et al. [43] have demonstrated that CNT strength, in particular, is very sensitive to clustering of vacancies (holes), which can lead to strength reductions of as much as 60% as compared to pristine tubes. In contrast, Sammalkorpi et al. [44] and Haskins et al. [45] have shown, through molecular dynamics (MD) simulations, that the tensile Young's Modulus of CNTs is much less sensitive to defects. Furthermore a small density of interlayer point defects, can significantly improve load transfer between adjacent CNT shells and tubes [21,37].

Irradiation induced point defects bridging graphitic layers can take several forms including; di-vacancy, interstitial, and Frenkel pair defects [41]. Telling et al. [41] demonstrated through first-principle quantum mechanics calculations, that in addition to interstitials atoms, effectively cross-linking adjacent graphitic layers, vacancies formed as a result of irradiation can also re-configure to covalently cross-link layers despite the relatively large atomic spacing of adjacent layers.

2.1.2. Knock on energy requirements

There are minimum energy requirements of the incident irradiation particle to knock out a carbon atom from the CNT lattice. A detailed discussion of these requirements can be found in a previous review article on irradiation of nanostructures [39]. Here we will briefly summarize the key points as related to irradiation of CNTs. The knock on threshold energy of an incoming particle is related to the displacement threshold energy (T_d) and the masses of the incoming particle (m_i) and a carbon atom (m_c) as follows [39]:

$$E_{th} = \frac{(m_i + m_c)^2}{4 m_c m_i} T_d \quad (1)$$

In the case of electron irradiation, due to the large relative mass of the carbon atom (m_c) as compared to the electron (m_e), the expression can be simplified to: $E_{th} \approx \frac{m_c}{4m_e} T_d$ suggesting that electrons with high kinetic energy are required to satisfy the threshold energy. This corresponds to threshold electron energies on the order of ~100 keV required to displace carbon atoms in the CNT lattice. More specifically the threshold energy is dependent on a number of factors including CNT diameter, chirality, angle of incidence between incoming electron and CNT lattice. Theoretical studies have predicted displacement threshold energies of ~15–22 eV [46–49] for incident electrons perpendicular to the CNT tube surface and as high as ~33–44 eV [47] for tangential incident electrons. Furthermore, small diameter CNTs are predicted to require lower displacement threshold than larger tubes [49]. These predicted displacement thresholds translate to required threshold electron energies of ranging from ~82 keV for small CNTs with electrons in a perpendicular configuration to as high as ~240 keV for large CNTs in a tangential configuration.

2.2. Electromagnetic irradiation

Another approach to enhancing shear interactions between adjacent CNTs within CNT fibers is by electromagnetic irradiation of polymer/CNT interfaces to bond polymer chains between adjacent CNTs. Unlike high energy particle irradiation, which creates covalent bonds directly between adjacent CNTs, electromagnetic irradiation can lead to either covalent bonding between polymer chains which bridge adjacent CNTs

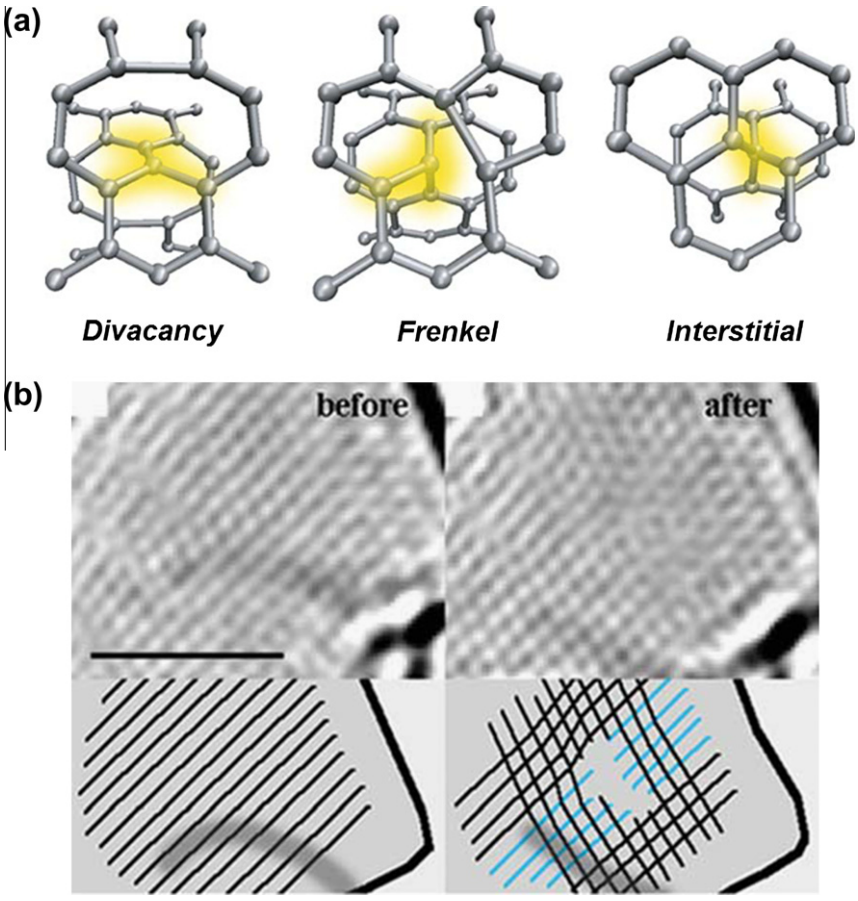

Fig. 2 – (a) Point defects bridging two shells of a DWCNT. Adapted from [21]. (b) HR-TEM images of a graphene layer before and after electron irradiation exhibiting the formation of an edge dislocation. Adapted from [42].

or the enhancement of interactions with interstitial molecules present between adjacent CNTs [50–54]. Polymer bridging, in the absence of irradiation induced cross-linking, has been utilized to enhance the ductility of CNT fibers [6], however, this approach can still lead to lower strength due to the absence of covalent bonds between polymer chains and CNTs. Strong covalent bonding between polymers chains that bridge the gaps between CNTs can be achieved by several electromagnetic irradiation methods. Ultraviolet (UV) irradiation has been demonstrated to induce covalent cross-linking in polymer/CNT materials such as layer-by-layer SWNT-poly (sodium 4-styenesulfonate) [54], and has been shown to increase shear interactions between interstitial dimethyl-formamide (DMF) molecules and CNTs [51]. Microwave irradiation has been shown to create very strong MWNT-polymer bonds to poly(ethylene terephthalate) (PET) and polycarbonate (PC) [53]. Finally, gamma irradiation can induce interstitial carboxyl like groups between adjacent CNTs which can potentially increase shear interactions [50].

3. Electron irradiation induced mechanical improvements at different length scales in CNT fibers

In the following sections we review recent theoretical and experimental demonstrations of the utilization of electron irradiation induced cross-links for mechanical improvements of fibers. A focus will be on applications at multiple length scales within fibers.

3.1. *Shells within MWCNTs*

Peng et al. [9] and Locascio et al. [21] demonstrated the effects of electron irradiation cross-linking through in situ TEM experiments conducted on MWCNTs irradiated using the electron beam (Fig. 3c). In these studies, it was found that only the outer shell of un-irradiated MWCNTs carried the tensile load prior to failure after which the outer shell slid with respect to the inner shell. As the irradiation levels increased, it was observed that multiple shells of the MWCNTs contributed to the load carrying capacity through shear load transfer to inner shells. Analysis of the true stress acting on the shells carrying load revealed that at low levels of irradiation the outer few CNT shells had a remarkable failure stress and modulus of ~100 GPa and ~1 TPa, respectively, whereas increased irradiation, which allowed corsslinking of many inner layers, led to a reduction in true strength and modulus to 35 GPa and 590 GPa, respectively [9].

MD and MM simulations of cross-linked DWCNTs have demonstrated that only a low density (~0.01–0.4 defects/Å) of irradiation induced point defects is required to approach theoretical limits of load transfer between the inner and outer

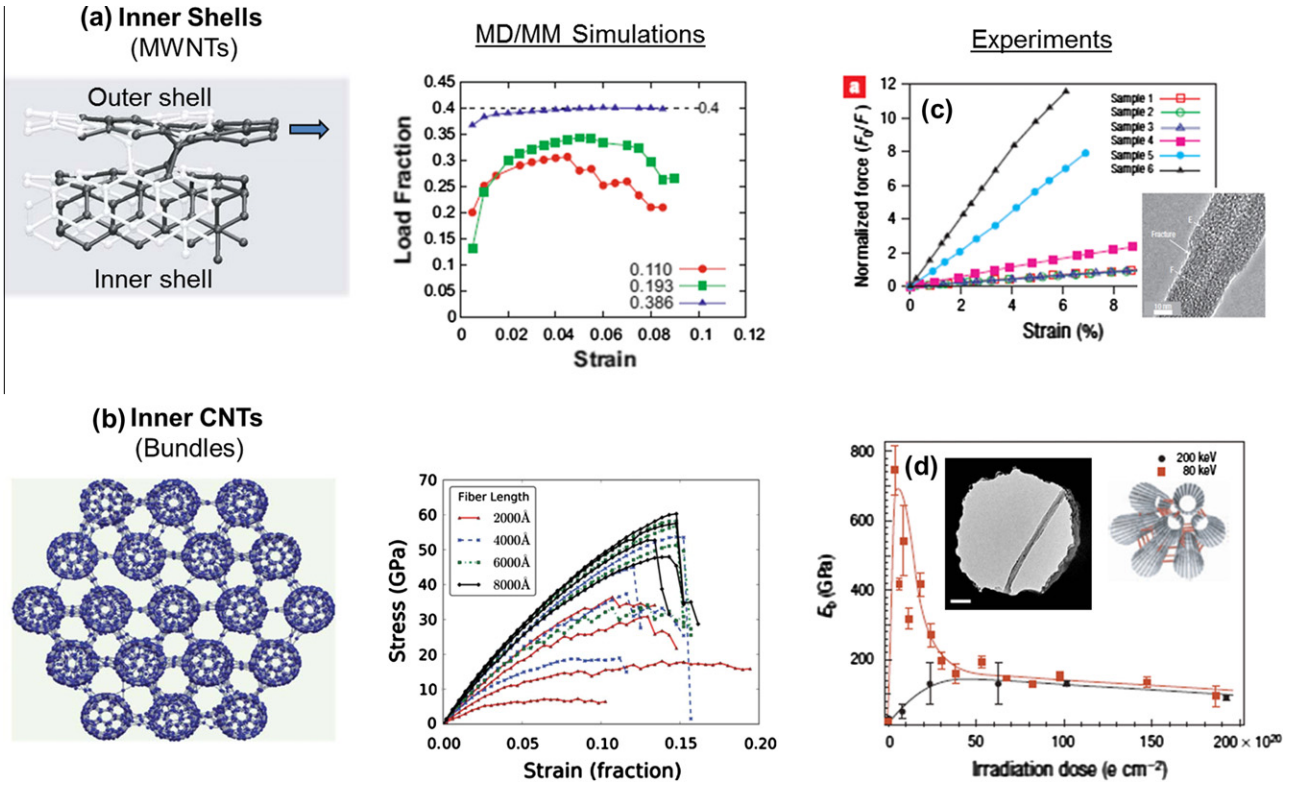

Fig. 3 – Atomistic simulations and experiments on electron induced crosslining in CNT materials. (a) Molecular mechanics simulations of cross-linking a DWCNT. Adapted from [21]. (b) Molecular dynamics simulations of cross-linking a SWCNT bundle. Adapted from [37]. (c) In-situ TEM experiments of cross-linking MWCNTs. Adapted from [9]. (d) AFM bending experiments on SWCNT bundles. Adapted from [29].

shells and increase the interlayer shear strength by orders of magnitude [21,55] (Fig. 3a). Both Huhtala et al. [55] and Locascio et al. [21] found that di-vacancy defects were more effective at increasing load transfer and interlayer shear strength as compared to interstitial defects, whereas Locascio et al. [21] also found that Frenkel defects were even more effective than the other two point defect types. Considering the experimental and theoretical findings of irradiation of MWCNTs suggest that control of defect density and distribution within the MWCNTs imparted by electron irradiation is a critical step in optimizing their mechanical behavior. Only a low density of cross-linking defects is required between each layer; however, achieving cross-link penetration, through many shells of a MWCNT, may lead to a high defect density on the outer shells and reduce their intrinsic strength and stiffness.

3.2. *CNTs within SWCNT bundles*

The next structural level in the hierarchy of CNT fibers is the interaction between adjacent CNTs within close packed bundles. At this level Kis et al. investigated the effects of electron irradiation induced cross-linking defects on enhancing the mechanical properties of SWCNT bundles by applying an AFM based deflection method [27,29] (Fig. 3d). In their study it was demonstrated that low doses ($\sim 5 \times 10^{20}$ e/cm^2) of electron irradiation at energies of 80 keV yielded a substantial increase in the effective bending modulus up to ~750 GPa [29]. Higher irradiation doses were found to significantly reduced the modulus, in this case to as low as ~100 GPa (at doses in excess of 40×10^{20} e/cm^2) due to the introduction of a high density of defects in the SWCNT shells and a transition to amorphous carbon structures. In addition, irradiation of electrons with higher beam energies (200 keV) was not found to lead to significant improvements in the bending stiffness. This is likely attributed to both the resolution in the control of the electron dose applied experimentally and the low resistance to high energy beam damage for SWCNT (as compared to MWCNTs) [39]. One limitation of the AFM bending based method is that it does not allow for a determination of the strength of the irradiated SWCNT bundles.

In the absence of experimental measurements, MD simulations of SWCNT bundles have provided insights into the achievable strength of irradiated bundles. Cornwell and Welch [37] conducted MD simulations of SWCNT bundles with a varying density of interstitial carbon atoms used to emulate interstitial defects created by electron irradiation (Fig. 3b). Here it was demonstrated that the strength of discontinues SWCNT bundles increased with cross-link density, with a strength of up to 62 GPa at the optimal cross-link density of ~0.7 nm^{-3}. The authors reported that this configuration consisted of 80.4 cross-links per CNT in the bundle which had a length of 8000 Å [37]. This corresponds to an interfacial linear cross-link density between each SWCNT of ~0.01 cross-links/Å. It is interesting to note that this optimal

cross-link density, between tubes in a bundle, is in a similar range to that found for the optimal cross-linking defect density, between shells in a MWCNT, as discussed in the previous section [21,55].

In addition to the cross-link density, the length of individual CNTs within a CNT fiber can also influence the strength of the fiber. MD simulations by Cornwell and Welch [37] predicted a high strength of ~50 GPa for cross-linked bundles with 8000 Å long CNTs with a cross-link density of only 0.1 nm^{-3}, whereas cross-linked bundles composed of 4000 Å long CNTs (with the same cross-sectional geometry) required a crosslink density of 0.7 nm^{-3} to achieve a similar strength. The implication of this finding is that CNT fibers composed of longer CNTs would require lower irradiation treatments (and hence a lower number of defects introduced) to achieve the same improvements in strength.

3.3. Cross-linking of shells and tubes within DWCNT bundles and CNT yarns

In the last two sections, cross-linking of shells within MWCNTs and cross-linking SWCNTs in bundles was discussed. Here we discuss a slightly more complex hierarchical CNT structure, double-walled carbon nanotube (DWCNT) bundles. This type of structure has two available levels of interfaces that can be cross-linked by electron irradiation; (1) the inner and outer shells within each DWCNT and (2) the adjacent DWCNTs within the bundle.

Filleter et al. [30] have conducted experimental studies on DCWNT bundles exposed to high energy electron irradiation in a TEM (Fig. 4). As mentioned above this material has two levels of hierarchy; inter tube shell-shell interactions as well as inter bundle tube-tube interactions, which can be cross-linked by irradiation. In this study it was found that both the effective strength and elastic modulus of the DWCNT bundles was increased by irradiation up to 17 GPa and 693 GPa respectively. The effective mechanical properties were determined by considering a crossectional area, which included the crossection of all tubes and shells with the DWCNT bundles where the typical CNT shell thickness of 0.33 nm was assumed. The number of tubes within each bundle was determined using a geometrical close packing model and HRTEM images of the fringe patterns of each individual bundle. The failure modes, identified from in situ TEM imaging, of the bundles were found to depend on the irradiation level. In the case of minimally irradiated bundles (0.5×10^{20} e/cm^2) the outer tubes within the bundles failed during the tensile test and slid with respect to the inner bundle of DWCNTs, akin to the sword-in-sheath failure observed for MWCNT shells. On the other hand, at optimal irradiation doses (~9–11×10^{20} e/cm^2) the bundles were found to fail across the entire cross section of shells and tubes confirming effective load transfer to the bundle interior.

In principle, the same mechanisms discussed above for cross-linking adjacent CNTs within bundles can be applied to cross-link the outer CNTs of adjacent CNT bundles. To date this has not been demonstrated directly as both experiments and simulations of the mechanical interactions between two isolated CNT bundles, for example, are difficult and time consuming. Initial demonstrations of the shear properties between isolated CNT bundles have been achieved for polymer cross-linked CNTs through in situ SEM and coarse-grain modeling methods [18]. A future direction in such studies will be to apply the same techniques to bundle-bundle junctions exposed to electron irradiation.

3.4. Comparison of electron beam energies and defect densities

As discussed in Section 3.2 the incident electron beam energy is an important criterion for inducing and controlling cross-linking defects in CNT fibers. The beam energy must be above a threshold of approximately 80 keV in order to create defects between shells and tubes [39]. Studies of MWCNTs have demonstrated that higher beam energies in the range of 100–200 keV can also be very effective at crosslining MWCNTs without significant degradation in the mechanical properties of the CNT shells themselves [9,30]. This, however, is not the case for SWCNTs that are less stable and can be rapidly degraded under higher energy electron beams [29,39]. Even higher electron beam energies of 1.25 MeV accompanied by heating has also been shown to bond multiple SWCNTs into continuous junctions [56], however it remains to be studied as to whether these modifications introduce significant defects and voids which can degrade the mechanical properties of the individual CNT shells.

A very important consideration in utilizing electron irradiation for enhancing the mechanical properties of CNT yarns is the optimization of the benefits of cross-linking to transfer load, and the detrimental effects of defect introduction into CNT shells. This tradeoff has been experimentally demonstrated in the context of both SWCNT and DWCNT bundles [29,30]. In these studies the optimal electron dose was found to be in a similar range of (~$5–10 \times 10^{20}$ e/cm^2). Furthermore, Kis et al. [29] demonstrated that at high levels of irradiation, the structure of SWCNT bundles is transformed into an amorphous carbon structure. This was supported by both TEM images of the resulting structures as well as bending moduli that approach that expected for amorphous carbon [29]. Raman spectroscopy investigations of CNTs irradiated with electrons have also demonstrated a transition to amorphous structures for high irradiation dose [57].

A key challenge that remains in connecting experimental demonstrations of cross-linking improvements in CNTs with theoretical predictions is a comparison of cross-linking defect densities. Experimentally, it is very difficult to measure or estimate the actual defect density imposed by electron beam irradiation. Most studies simply report on the variation in mechanical properties with the electron dose (typically in e^-/cm^2). While this specifies the flux of electrons passing though the material, the density of cross-linking defects formed by the electron beam depends on a number of other factors which include the electron energy, the curvature of the CNT shells, the thickness of the CNT material, and the mean free path of electron in the graphitic material. Although this may be difficult to determine experimentally, direct comparison between experiments and atomistic simulations can be used in the future to achieve insights into the experimental defect densities and help guide optimization of mechanical properties. This will require modeling CNT systems that

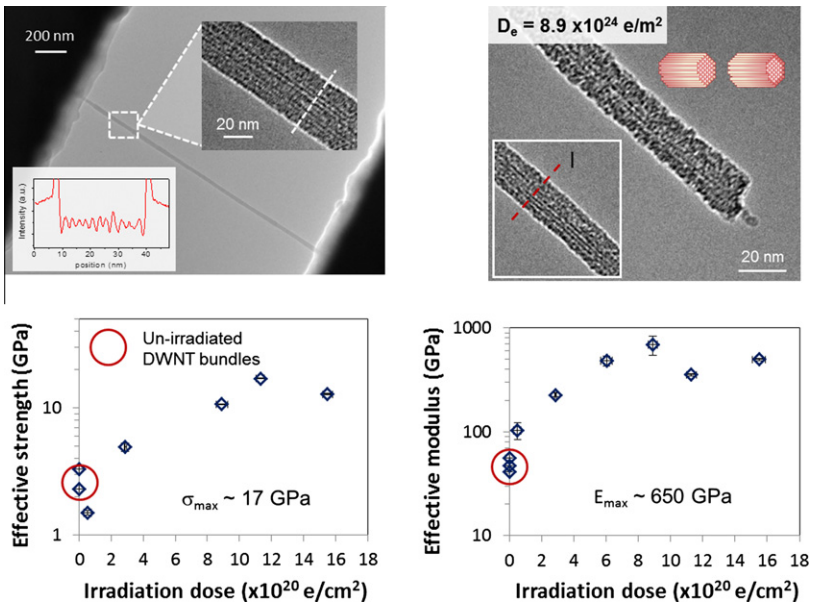

Fig. 4 – Electron irradiation strengthening of double-walled carbon nanotube bundles. (Top) In-situ TEM images of DWCNT bundles tested using a MEMS based tensile testing technique. (Bottom) Effective strength and tensile modulus as a function of irradiation dose for different DWCNTs. Adapted from [30].

match those found in experiments. This requirement is in principle already achievable as MD simulations have already been demonstrated for SWCNT bundles (d_{bundle} = ~5 nm, d_{cnt} = ~0.7 nm N_{cnt} = 19, l = ~800 nm [37]), which approach sizes that have been tested experimentally (d_{bundle} = ~10 nm, d_{cnt} = ~2.5 nm, N_{cnt} = 14, l = ~2600 nm [30]).

4. Application of irradiation cross-linking to macroscopic CNT yarns

Macroscopic CNT based yarns and fibers have been realized using a number of different synthesis techniques, most notably, direct spinning in situ [20,58] and post spinning of CVD grown mats [6] and spinning continuously draw CNT mats from forests [3]. While these methods produce CNT fibers with good mechanical properties, such as typical strengths of ~1 GPa, they do not take advantage of CNT cross-linking. Several studies have applied irradiation techniques to cross-link macroscopic CNT yarns and buckypapers [50,51,59]. Miao et al. [50] used gamma irradiation to introduce increased lateral interactions between CNTs within yarns spun from CNT forests. Improvements in strength and stiffness of the yarns were observed with irradiation, however no clear trend with increasing irradiation level was observed (Fig. 5). The improvements were attributed to the formation of carboxyl like groups between adjacent CNTs due to gamma-irradiation induced oxidation of the CNTs not by direct CNT-CNT cross-linking. Ultraviolet (UV) light irradiation has also been applied to cross-link CNT yarns by Miko et al. [51]. In this study increases in both the elastic modulus and electrical conductivity were observed following UV irradiation. Here, similar to the case of gamma-irradiation, the cross-linking was not in the form of direct CNT covalent cross-linking of carbon atoms, but instead by a UV initiated side reaction between surface functional groups on the CNTs and DMF molecules present from the original CNT suspension.

4.1. *Key challenges: current density and electron penetration depth*

The application of electron irradiation for directly cross-linking adjacent CNTs within macroscopic CNT yarns and fibers remains to be studied. The two key challenges in achieving successful macroscopic cross-linking are; (1) applying a high enough current density over a large area in order to approach the irradiation doses used in smaller scale studies, and (2) addressing the issue of limited electron penetration depth in order to achieve uniform irradiation over the entire cross-sectional area of macroscopic fibers. As discussed in Section 3 the irradiation doses found to be optimal for cross-linking CNTs and CNT bundles lie in the range of ~5–10 × 10^{20} e/cm^2. In the TEM setup used for these experiments, the current density was varied in the range of 0.3–2 A/cm^2 [29,30], which allowed the optimal doses to be delivered in a matter of seconds or minutes. In contrast, industrial scale electron irradiation equipment which is capable of delivering electron beams which spread over large areas of mm or inches, typically operate on the order of ~μA/cm^2. Under such conditions it would require days or months to irradiate a single CNT yarn sample to a comparable dose, as the dose rate would be orders of magnitude lower. Even for low Z elements (such as carbon) the penetration depth of 200 keV electrons is <1 μm. Therefore the electron beam will not be able to penetrate the entire crossection of macroscopic CNT fibers which typically have a diameter of 10–100 μm.

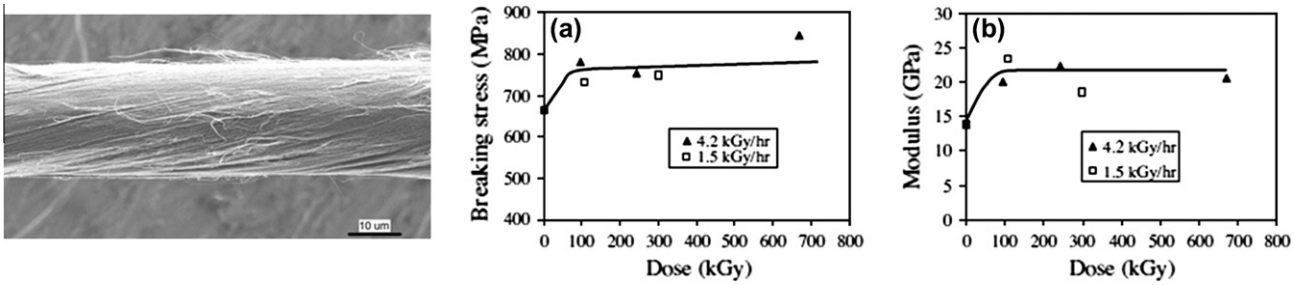

Fig. 5 – Gamma-irradiation of CNT yarns. (left) SEM image of a CNT yarn spun from a CNT forest. (right) Strength and elastic modulus of CNT yarns exposed to different levels of gamma-irradiation. Adapted from [50].

4.2. *Manufacturing approaches: continuous spinning fabrication*

To address the above limitations novel approaches will need to be applied for future studies. The issue of penetration depth can in principle be addressed by integrating in situ CVD spinning or spinning from a CNT forest with an electron irradiation setup such that a thin mat of CNTs are irradiated prior to final spinning into a fiber or yarn. This would enable complete irradiation of a thin (~1 μm) CNT mat which will then be the precursor to the macroscopic CNT fiber. The limitation of electron beam current density is more difficult as achieving a high density electron beam over a large area is technically challenging. One possible approach would be to conduct irradiation experiments at elevated temperature to reduce the barrier to the formation of covalent cross-linking between CNTs, which may require a lower electron irradiation dose to achieve comparable cross-linking density. Other approaches such as plasma irradiation are also possible[1].

5. Summary

We have reviewed the application of irradiation for cross-linking fibers and yarns based on CNTs, which are possible candidates as reinforcement elements in composite materials. Electron irradiation, in particular, has been demonstrated through proof of principle studies to be effective in creating strong and stiff covalent bonds between the outer walls of adjacent CNTs and between the internal walls of MWCNTs, which lead to improvements in mechanical performance. Experiments and simulations on multiple length scales, from shells within individual MWCNTs to adjacent DWCNTs within bundles, have shown orders of magnitude improvements in strength and stiffness as a result of irradiation. A common observation in the studies is a balance between the benefits of shell cross-linking and the disadvantage of introducing defects in the CNT walls. Initial studies on applying irradiation cross-linking strategies to macroscopic CNT yarns and fibers are beginning to reveal the benefits of the approach. However, strategies using electron irradiation on macroscopic samples face two key obstacles in applying high current densities and achieving optimal electron penetration depths.

[1] C. Welch, private communication, 2012.

Acknowledgments

The authors gratefully acknowledge support from ARO through MURI award No. W911NF-09-1-0541 and from NSF through award No. DMR-0907196.

REFERENCES

[1] Koziol K, Vilatela J, Moisala A, Motta M, Cunniff P, Sennett M, et al. High-performance carbon nanotube fiber. Science 2007;318(5858):1892–5.
[2] Motta M, Moisala A, Kinloch I, Windle A. High performance fibres from dog bone carbon nanotubes. Adv Mater 2007;19:3721–6.
[3] Zhang M, Atkinson KR, Baughman RH. Multifunctional carbon nanotube yarns by downsizing an ancient technology. Science 2004;306(5700):1358–61.
[4] Dalton AB, Collins S, Munoz E, Razal JM, Ebron VH, Ferraris JP, et al. Super-tough carbon-nanotube fibres-these extraordinary composite fibres can be woven into electronic textiles. Nature 2003;423(6941):703–6.
[5] Li Y-L, Kinloch I, Windle A. Direct spinning of carbon nanotube fibers from chemical vapor deposition synthesis. Science 2004;304:276–8.
[6] Naraghi M, Filleter T, Moravsky A, Locascio M, Loutfy RO, Espinosa HD. A multiscale study of high performance double-walled nanotube-polymer fibers. ACS Nano 2010;4(11):6463–76.
[7] Wu AS, Chou T-W. Carbon nanotube fibers for advanced composites. Mater Today 2012;15:302–10.
[8] Espinosa HD, Filleter T, Naraghi M. Multiscale experimental mechanics of hierarchical carbon-based materials. Adv Mater 2012;24(21):2805–23.
[9] Peng B, Locascio M, Zapol P, Li S, Mielke SL, Schatz GC, et al. Measurements of near-ultimate strength for multiwalled carbon nanotubes and irradiation-induced crosslinking improvements. Nat Nanotechnol 2008;3(10):626–31.
[10] Yu MF, Lourie O, Dyer MJ, Moloni K, Kelly TF, Ruoff RS. Strength and breaking mechanism of multiwalled carbon nanotubes under tensile load. Science 2000;287(5453):637–40.
[11] Girifalco LA, Lad RA. Energy of cohesion, compressibility, and the potential energy functions of the graphite system. J Chem Phys 1956;25(4):693–7.
[12] Kis A, Jensen K, Aloni S, Mickelson W, Zettl A. Interlayer forces and ultralow sliding friction in multiwalled carbon nanotubes. Phys Rev Lett 2006;97(2).

[13] Chopra NG, Benedict LX, Crespi VH, Cohen ML, Louie SG, Zettl A. Fully collapsed carbon nanotubes. Nature 1995;377(6545):135–8.
[14] Zacharia R, Ulbricht H, Hertel T. Interlayer cohesive energy of graphite from thermal desorption of polyaromatic hydrocarbons. Phys Rev B 2004;69:155406.
[15] Yu MF, Yakobson BI, Ruoff RS. Controlled sliding and pullout of nested shells in individual multiwalled carbon nanotubes. J Phys Chem B 2000;104(37):8764–7.
[16] Kalantar J, Drzal LT. The bonding mechanism of aramid fibers to epoxy matrices.1. A review of the literature. J Mater Sci 1990;25(10):4186–93.
[17] Cumings J, Zettl A. Low-friction nanoscale linear bearing realized from multiwall carbon nanotubes. Science 2000;289(5479):602–4.
[18] Naraghi M, Bratzel G, Filleter T, An Z, Wei X, S.T.Nguyen, et al. Atomistic investigation of load transfer between DWNT bundles croslinked by PMMA-oligomers. Adv Func Mater 2012. http://dx.doi.org/10.1002/adfm.201201358.
[19] Ke CH, Zheng M, Zhou GW, Cui WL, Pugno N, Miles RN. Mechanical peeling of free-standing single-walled carbon-nanotube bundles. Small 2010;6(3):438–45.
[20] Li Y-L, Kinloch IA, Windle AH. Direct spinning of carbon nanotube fibers from chemical vapor deposition synthesis. Science 2004;304(5668):276–8.
[21] Locascio M, Peng B, Zapol P, Zhu Y, Li S, Belytschko T, et al. Tailoring the load carrying capacity of MWCNTs through inter-shell atomic bridging. Exp Mech 2009;49(2):169–82.
[22] Filleter T, Yockel S, Naraghi M, Paci JT, Compton OC, Mayes ML, et al. Experimental-computational study of shear interactions within double-walled carbon nanotube bundles. Nano Lett 2012;12(2):732–42.
[23] Yu MF, Files B, Arepalli S, Ruoff R. Tensile loading of ropes of single wall carbon nanotubes and their mechanical properties. Phys Rev Lett 2000;84(24):5552–5.
[24] Wei XD, Naraghi M, Espinosa HD. Optimal length scales emerging from shear load transfer in natural materials: application to carbon-based nanocomposite design. ACS Nano 2012;6(3):2333–44.
[25] Yang TY, Zhou ZR, Fan H, Liao K. Experimental estimation of friction energy within a bundle of single-walled carbon nanotubes. Appl Phys Lett 2008;93(4).
[26] Banhart F. The formation of a connection between carbon nanotubes in an electron beam. Nano Lett 2001;1(6):329–32.
[27] Ajayan PM, Banhart F. Strong bundles. Nat Mater 2004;3(3):135–6.
[28] Krasheninnikov AV, Banhart F. Engineering of nanostructured carbon materials with electron or ion beams. Nat Mater 2007;6(10):723–33.
[29] Kis A, Csanyi G, Salvetat JP, Lee TN, Couteau E, Kulik AJ, et al. Reinforcement of single-walled carbon nanotube bundles by intertube bridging. Nat Mater 2004;3(3):153–7.
[30] Filleter T, Bernal R, Li S, Espinosa HD. Ultra high strength and stiffness in cross-linked hierarchical carbon nanotube bundles. Adv Mater 2011;23:2855–60.
[31] Simmons. Radiation damage in graphite. London: Pergamon; 1965.
[32] Thrower PA. The study of defects in graphite by transmission electron microscopy. Chem Phys Carbon 1969;5:217–319.
[33] Goggin PR. Some Effects of Electron Irradiation on Youngs Modulus of Graphite. Nature 1963;199(4891):367–8.
[34] Leroy G, Temsamani DR, Sana M, Wilante C. Refinement and extension of the table of standard energies for bonds involving hydrogen and various atoms of group-IV to group-vii of periodic-table. J Mol Struct 1993;300:373–83.
[35] Schabel MC, Martins JL. Energetics of interplanar binding in graphite. Phys Rev B 1992;46(11):7185–8.
[36] Astrom JA, Krasheninnikov AV, Nordlund K. Carbon nanotube mats and fibers with irradiation-improved mechanical characteristics: a theoretical model. Phys Rev Lett 2004;93(21):4.
[37] Cornwell CF, Welch CR. Very-high-strength (60-GPa) carbon nanotube fiber design based on molecular dynamics simulations. J Chem Phys 2011;134(20).
[38] Hong WK, Lee C, Nepal D, Geckeler KE, Shin K, Lee T. Radiation hardness of the electrical properties of carbon nanotube network field effect transistors under high-energy proton irradiation. Nanotechnology 2006;17(22):5675–80.
[39] Krasheninnikov AV, Nordlund K. Ion and electron irradiation-induced effects in nanostructured materials. J Appl Phys 2010;107(7).
[40] Banhart F. Irradiation effects in carbon nanostructures. Rep Prog Phys 1999;62(8):1181–221.
[41] Telling RH, Ewels CP, El Barbary AA, Heggie MI. Wigner defects bridge the graphite gap. Nat Mater 2003;2(5):333–7.
[42] Hashimoto A, Suenaga K, Gloter A, Urita K, Iijima S. Direct evidence for atomic defects in graphene layers. Nature 2004;430(7002):870–3.
[43] Mielke SL, Troya D, Zhang S, Li JL, Xiao SP, Car R, et al. The role of vacancy defects and holes in the fracture of carbon nanotubes. Chem Phys Lett 2004;390(4–6):413–20.
[44] Sammalkorpi M, Krasheninnikov A, Kuronen A, Nordlund K, Kaski K. Mechanical properties of carbon nanotubes with vacancies and related defects. Phys Rev B 2004;70(24):245416.
[45] Haskins RW, Maier RS, Ebeling RM, Marsh CP, Majure DL, Bednar AJ, et al. Tight-binding molecular dynamics study of the role of defects on carbon nanotube moduli and failure. J Chem Phys 2007;127(7):074708.
[46] Smith BW, Luzzi DE. Electron irradiation effects in single wall carbon nanotubes. J Appl Phys 2001;90(7):3509–15.
[47] Crespi VH, Chopra NG, Cohen ML, Zettl A, Louie SG. Anisotropic electron-beam damage and the collapse of carbon nanotubes. Phys Rev B 1996;54(8):5927–31.
[48] Krasheninnikov AV, Banhart F, Li JX, FA S, Nieminen RM. Stability of carbon nanotubes under electron irradiation; role of tube diameter and chirality. Phys Rev B 2005;72(12):125428.
[49] Banhart F, Li JX, Krasheninnikov AV. Carbon nanotubes under electron irradiation: stability of the tubes and their action as pipes for atom transport. Phys Rev B 2005;71(24).
[50] Miao MH, Hawkins SC, Cai JY, Gengenbach TR, Knott R, Huynh CP. Effect of gamma-irradiation on the mechanical properties of carbon nanotube yarns. Carbon 2011;49(14):4940–7.
[51] Miko C, Milas M, Seo JW, Gaal R, Kulik A, Forro L. Effect of ultraviolet light irradiation on macroscopic single-walled carbon nanotube bundles. Appl Phys Lett 2006;88(15):151905.
[52] Miko C, Milas M, Seo JW, Gaal R, Kulik A, Forro L. Effect of ultraviolet light irradiation on macroscopic single-walled carbon nanotube bundles. Appl Phys Lett 2006;88(15).
[53] Wang CY, Chen TG, Chang SC, Cheng SY, Chin TS. Strong carbon-nanotube-polymer bonding by microwave irradiation. Adv Funct Mater 2007;17(12):1979–83.
[54] Qin SH, Qin DQ, Ford WT, Zhang YJ, Kotov NA. Covalent cross-linked polymer/single-wall carbon nanotube multilayer films. Chem Mater 2005;17(8):2131–5.
[55] Huhtala M, Krasheninnikov AV, Aittoniemi J, Stuart SJ, Nordlund K, Kaski K. Improved mechanical load transfer between shells of multiwalled carbon nanotubes. Phys Rev B 2004;70(4):045404.
[56] Terrones M, Banhart F, Grobert N, Charlier J-C, Terrones H, Ajayan PM. Molecular junctions by joining single-walled carbon nanotubes. Phys Rev Lett 2002;89(7):075505.
[57] McDonell K, Proust G, Shen LM. Effects of electron irradiation on single-walled carbon nanotubes. Iop Conf Ser-Mat Sci 2010:10.

[58] Stano KL, Koziol K, Pick M, Motta MS, Moisala A, Vilatela JJ, et al. Direct spinning of carbon nanotube fibers from liquid feedstock. Int J Mater Form 2008;1:4.

[59] Skakalova V, Hulman M, Fedorko P, Lukac P, Roth S. Effect of gamma-irradiation on single-wall carbon nanotube paper. AIP Conf Proc 2003;685:143–7.